Parallel Perturbed Gauss-Newton State Estimator Based on Fortescue Transformation for Unbalanced Power Systems

Izudin Džafić, *Senior Member*, *IEEE*

***Abstract*—This letter extends the complex-variable perturbed Gauss-Newton method to estimate the state of unbalanced power systems by exploiting the Fortescue transformation. It proposes a novel and efficient graph-based way to deal with singularities due to zero-sequence network parts bounded with delta transformer windings and isolated from the ground. The estimator can handle both phasor and complex power measurements. Compared with the standard complex-variable unbalanced state estimator, it achieves better numerical stability and a speed-up of around three times using a sequential implementation and five times using parallel execution.**

***Index Terms*—Delta-winding, Fortescue transformation, iterative algorithm, least-squares approximation, parallel algorithm, perturbation methods, ill-conditioning, state estimation, symmetrical component.**

I. Introduction

THERE is an increasing interest in the fast solution of large-scale state estimation problems emanating from many sensors in broad geographical areas involved in market transactions. Furthermore, considering renewables that are primarily connected at the sub-transmission level requires the modeling of unbalanced loading in the state estimator, thus further increasing the computational burden of this real-time function [1]. Reference [2] proposed alleviating the speed bottleneck through modal decoupling, and [3] exploited the use of compensation to account for untransposed lines and unsymmetrical construction. However, both [2] and [3] considered networks measured only by phasor measurement units (PMUs), while the sensors in existing networks can be either the modern PMUs or part of the legacy supervisory control and data acquisition (SCADA) system. Reference [4] presented a practical multiphase distribution state estimation method that included legacy SCADA measurements and used symmetrical components. The method has been tested on multi-phase distribution networks with grounded neutral points. Using the pseudo Gauss-Newton framework, [5] demonstrated how SCADA measurements, in addition to PMUs, could be integrated into the Fortescue-based estimator with different transformer connection types. It is assumed that buffering can manage the discrepancy between SCADA and PMU refresh rates by identifying the phasor measurement values employed in the hybrid estimator solution [6]. The paper also discussed the different transformer connections that give rise to isolation from the ground in the zero-sequence model, and presented zero-sequence island detection that permits stable matrix factorization. This letter has two main contributions: ① a graph-based algorithm that fully exploits Fortescue transformation on physically symmetrical three-phase networks with unbalanced loading and avoids matrix singularity introduced by the delta windings; ② a parallel algorithm that utilizes the natural decomposition of Fortescue components and results in a speed-up of up to five times compared with the conventional phase-coordinates method [7]. These two improvements are essential for the real-time tracking of the source of imbalance in transmission networks.

The algorithm proposed herein mainly targets transmission networks. It can be applied to large European cities where the distribution network is constructed by cables, giving a three-phase symmetrical structure [8]. The proposed algorithm based on the Fortescue transformation can be applied to multi-phase networks comprised of symmetrical three-phase, two-phase, and one-phase network parts. Still, it requires the Fortescue transformation for two-phase and single-phase branches as described in [9], [10]. However, if the three-phase and two-phase network components are asymmetric, the asymmetry must be compensated by employing fictitious current generators on both sides of the branch [11].

II. State Estimator Based on Fortescue Transformation

The proposed algorithm combines the pseudo Gauss-Newton state estimation (PGNSE) algorithm [5] with the Fortescue transformation to account for unbalanced loading. First, complex branch and injected power measurements are converted to phase branch and injected *abc*-phasor currents $\boldsymbol{x}^{(abc)}$ using the most recent estimates of the *abc*-phasor voltages.

Manuscript received: June 9, 2022; revised: June 23, 2022; accepted: July 15, 2022. Date of CrossCheck: July 15, 2022. Date of online publication: July 26, 2022.

The work of I. Džafić was supported by MONKS, Sarajevo, FBiH, Bosnia and Herzegovina (No. 27-02-11-41250-34/21).

I. Džafić (corresponding author) is with the Faculty of Electrical Engineering, University of Sarajevo, Sarajevo 71000, Bosnia and Herzegovina (e-mail: idžafić@etf.unsa.ba).

DOI: 10.35833/MPCE.2022.000342

These currents are then converted to 012-phasor currents $\boldsymbol{x}^{(012)}$ using the Fortescue analysis equations in (1) and (2). The PMU voltage and current measurements can be transferred to symmetrical components without any adjustment.

$$\boldsymbol{x}^{(012)} = \boldsymbol{T}_{(abc)}^{(012)} \boldsymbol{x}^{(abc)} \tag{1}$$

$$\begin{cases} \boldsymbol{T}_{(abc)}^{(012)} = \dfrac{1}{3}\begin{bmatrix} 1 & 1 & 1 \\ 1 & \alpha & \alpha^2 \\ 1 & \alpha^2 & \alpha \end{bmatrix} \\ \alpha = \mathrm{e}^{\mathrm{j}\frac{2\pi}{3}} \end{cases} \tag{2}$$

After converting active and reactive power measurement pairs to complex voltage and current counterparts, a PGNSE formulation for each Fortescue component $f \in \{0, 1, 2\}$ is established:

$$\begin{bmatrix} (\overline{\boldsymbol{H}}^{(f)})^{\mathrm{T}} \boldsymbol{W} \boldsymbol{H}^{(f)} & (\overline{\boldsymbol{E}}^{(f)})^{\mathrm{T}} \\ \boldsymbol{E}^{(f)} & \boldsymbol{0} \end{bmatrix} \begin{bmatrix} \boldsymbol{v}^{(f)} \\ \boldsymbol{\lambda}^{(f)} \end{bmatrix} = \begin{bmatrix} (\overline{\boldsymbol{H}}^{(f)})^{\mathrm{T}} \boldsymbol{W} \hat{\boldsymbol{z}}^{(f)} \\ \boldsymbol{0} \end{bmatrix} \tag{3}$$

In a power system with nN nodes, nM real-time measurements, and nZ zero injection measurements, $\boldsymbol{H}$ is a complex measurement Jacobian matrix with dimension $nM \times (nN)$; $\boldsymbol{W}$ is a diagonal real valued matrix of measurement weighting factors with dimension $nM \times (nM)$; $\hat{\boldsymbol{z}}$ is a complex vector with dimension $nM \times 1$; $\boldsymbol{E}$ is the equality constraints matrix for zero-injection measurements; $\boldsymbol{v}$ is the vector of complex node voltages with dimension $nN \times 1$; and $\boldsymbol{\lambda}$ is the vector of Lagrange multipliers with dimension $nZ \times 1$. The overbar "–" indicates the complex conjugate and the hat "^" is for quantities derived from measurements.

A. Measurement Model in Fortescue Coordinates

This subsection defines entries in the complex measurement Jacobian matrix $\boldsymbol{H}$ and right hand size vector $\hat{\boldsymbol{z}}$ for each Fortescue component *f*. Measurements are assumed to be connected on node *p* in the case of injection measurements or on terminal *p* when located on a branch connecting nodes *p* and *n*. Measurements of power, current, and zero injection necessitate the use of the complex system admittance matrix $\boldsymbol{Y}$. Power and current measurements on a branch require π-equivalent entries denoted by $\boldsymbol{y}$. For each Fortescue component *f*, the dimension of the matrix $\boldsymbol{Y}$ is $nN \times (nN)$ and the dimension of the matrix $\boldsymbol{y}$ is 2×2. The set of nodes connected to node *p* is denoted by β_p.

1) Voltage PMU

The measurement number is *m* measured at node *p*. Equation (2) converts a phase-to-ground real-time voltage measurement $\hat{\boldsymbol{v}}_p^{(abc)}$ to Fortescue $\hat{\boldsymbol{v}}_p^{(012)}$. Following that, the respective entries of the vector $\hat{\boldsymbol{z}}$ and the matrix $\boldsymbol{H}$ are obtained:

$$\hat{z}_m^{(f)} = \hat{v}_p^{(f)} \tag{4}$$

$$H_{m,p}^{(f)} = 1 \tag{5}$$

Special attention must be paid to the slack (reference) angle in order to keep the problem solvable. There are two approaches to modeling the reference angle condition [7], [12]. The first approach uses a single global positioning system (GPS) reference for all nodal voltages, and the slack node voltage measurement is modeled in the same way as any other PMU voltage measurement. The second approach employs a bus *p* as the reference, with the slack angle condition accounted for by making the angle of $u_p^{(a)} = 0°$, $u_p^{(b)} = -120°$, and $u_p^{(c)} = 120°$.

2) Branch Current PMU

The measurement number is *m* from node *p* to node *n*. Equation (2) converts a phase-to-ground real-time current measurement $\hat{\boldsymbol{i}}_p^{(abc)}$ to Fortescue $\hat{\boldsymbol{i}}_p^{(012)}$. Entries of the vector $\hat{\boldsymbol{z}}$ and the matrix $\boldsymbol{H}$ are obtained as:

$$\hat{z}_m^{(f)} = \hat{i}_{p,n}^{(f)} \tag{6}$$

$$H_{m,j}^{(f)} = \begin{cases} y_{p,p}^{(f)} & j = p \\ y_{p,n}^{(f)} & j = n \\ 0 & \text{otherwise} \end{cases} \tag{7}$$

3) Injected Current PMU

The measurement number is *m* injected at node *p*. Similarly, by applying (2), measured phasor currents can be converted to the Fortescue domain. The required entries are as follows:

$$\hat{z}_m^{(f)} = \hat{i}_p^{(f)} \tag{8}$$

$$H_{m,j}^{(f)} = \begin{cases} Y_{p,p}^{(f)} & j = p \\ Y_{p,n}^{(f)} & j = n \wedge n \in \beta_p \\ 0 & \text{otherwise} \end{cases} \tag{9}$$

4) Branch Complex Power

The measurement number is *m* from node *p* to node *n*. Using previously calculated complex voltages at node *p*, phase complex powers are converted to Fortescue complex currents:

$$\hat{\boldsymbol{i}}_{p,n}^{(012)} = \boldsymbol{T}_{(abc)}^{(012)} \begin{bmatrix} \dfrac{\overline{s}_{p,n}^{(a)}}{\overline{v}_p^{(a)}} & \dfrac{\overline{s}_{p,n}^{(b)}}{\overline{v}_p^{(b)}} & \dfrac{\overline{s}_{p,n}^{(c)}}{\overline{v}_p^{(c)}} \end{bmatrix}^{\mathrm{T}} \tag{10}$$

where *s* is the complex power. After conversion, populating the right hand side vector $\hat{\boldsymbol{z}}$ and the matrix $\boldsymbol{H}$ is identical to the case with injected PMU current measurement (6) and (7).

5) Injected Complex Power

The measurement number is *m* injected at node *p*. This measurement type also necessitates a conversion step based on the previously calculated node voltages in phase coordinates, as shown in (11). The required entries are the same as (8) and (9).

$$\hat{\boldsymbol{i}}_p^{(012)} = \boldsymbol{T}_{(abc)}^{(012)} \begin{bmatrix} \dfrac{\overline{s}_p^{(a)}}{\overline{v}_p^{(a)}} & \dfrac{\overline{s}_p^{(b)}}{\overline{v}_p^{(b)}} & \dfrac{\overline{s}_p^{(c)}}{\overline{v}_p^{(c)}} \end{bmatrix}^{\mathrm{T}} \tag{11}$$

6) Voltage Magnitude

The measurement number is *m* measured at node *p*. The right hand side for this measurement was made complex-valued by rotating a real-valued measurement by angle of the previously calculated voltage in Fortescue coordinates:

$$\hat{z}_m^{(f)} = \left| \hat{v}_p^{(f)} \right| \angle v_p^{(f)} \tag{12}$$

$$H_{m,p}^{(f)} = 1 \tag{13}$$

7) Zero Injection

The measurement number is *m* measured at node *p*. The entries of the matrix $\boldsymbol{E}$ (equality constraints) are calculated using the system admittance matrix $\boldsymbol{Y}$ as follows:

$$E_{m,j}^{(f)}=\begin{cases}Y_{p,p}^{(f)} & j=p\\ Y_{p,n}^{(f)} & j=n\wedge n\in\beta_p\\ 0 & \text{otherwise}\end{cases} \tag{14}$$

B. Solution Procedure

The obtained estimation subsystems for positive, negative, and zero sequences can be solved sequentially or in parallel [13] with the factorized Jacobian matrices. Figure 1 shows the sequential and parallel PGNSE algorithm using Fortescue transformation for state estimation of symmetrical transmission networks with unbalanced loading. In Fig. 1, the zero-, positive-, and negative-sequence quantities are denoted by $f=0$, 1, and 2, respectively; $\hat{i}_{m,n}^{(\varphi)}$ is the phasor current at node/branch m in iteration n for phase φ; $\hat{\boldsymbol{i}}_{m,n}^{(abc)}$ is the vector of *abc*-phasor currents at node/branch m in iteration n; $\hat{\boldsymbol{i}}_{m,n}^{(012)}$ is the vector of 012-phasor currents at node/branch m in iteration n; $\boldsymbol{G}^{(f)}$ is the gain matrix; $\boldsymbol{J}^{(f)}$ is the Jacobian matrix; $\hat{s}_m^{(\varphi)}$ is the complex power at node/branch m for phase φ; S_{sl} is the set of slack nodes; $\boldsymbol{v}_n^{(f)}$ is the phasor voltage vector in iteration n; $\boldsymbol{v}_{p,n}^{(abc)}$ is the vector of *abc*-phasor voltages at node p in iteration n; and $\boldsymbol{Y}^{(f)}$ is the modified nodal admittance matrix. It is important to note that the weight matrix entries corresponding to legacy measurements must be adjusted [4], [14]-[16].

In PGNSE algorithm, the sequence Jacobian matrices $\boldsymbol{J}^{(k)}$ are calculated and factorized only once, giving rise to efficient computation. Unlike the positive- and negative-sequence networks, the zero-sequence network will contain one or more islands that are conductively isolated from the ground giving rise to a singular zero-sequence Jacobian matrix [17]. The following section discusses the transformer model in sequence networks as it is the reason for the existence of zero-sequence islands and the associated singularity of the complete Jacobian matrix.

III. Transformer Model

The short-circuit and open-circuit tests are typical procedures to establish the π-equivalent circuit of a transformer. In case of unbalanced loading, it is necessary to adequately address zero-sequence modeling and the impact of the clock number of the transformer.

A. Positive- and Negative-sequence Transformer Circuits

Figure 2 is the general π-equivalent circuit applied to the positive-sequence models for all transformers. Since the transformer connection introduces a phase shift between primary and secondary phase voltages, the transformer ratio is defined as a complex number (15), where c is the so-called clock number [18].

$$t=|t|\mathrm{e}^{\mathrm{j}c\frac{\pi}{6}} \tag{15}$$

There are two possible clock numbers ($c=0, 6$) for the wye-wye transformer, and for the wye-delta and delta-wye connections, there are four possible numbers ($c=1, 5, 7, 11$). The clock numbers form part of the transformer designation: *Yyc*, *Ydc*, and *Dyc*. Equation (16) represents the transformer positive-sequence nodal equations for the π-equivalent circuit in Fig. 2 after eliminating node x.

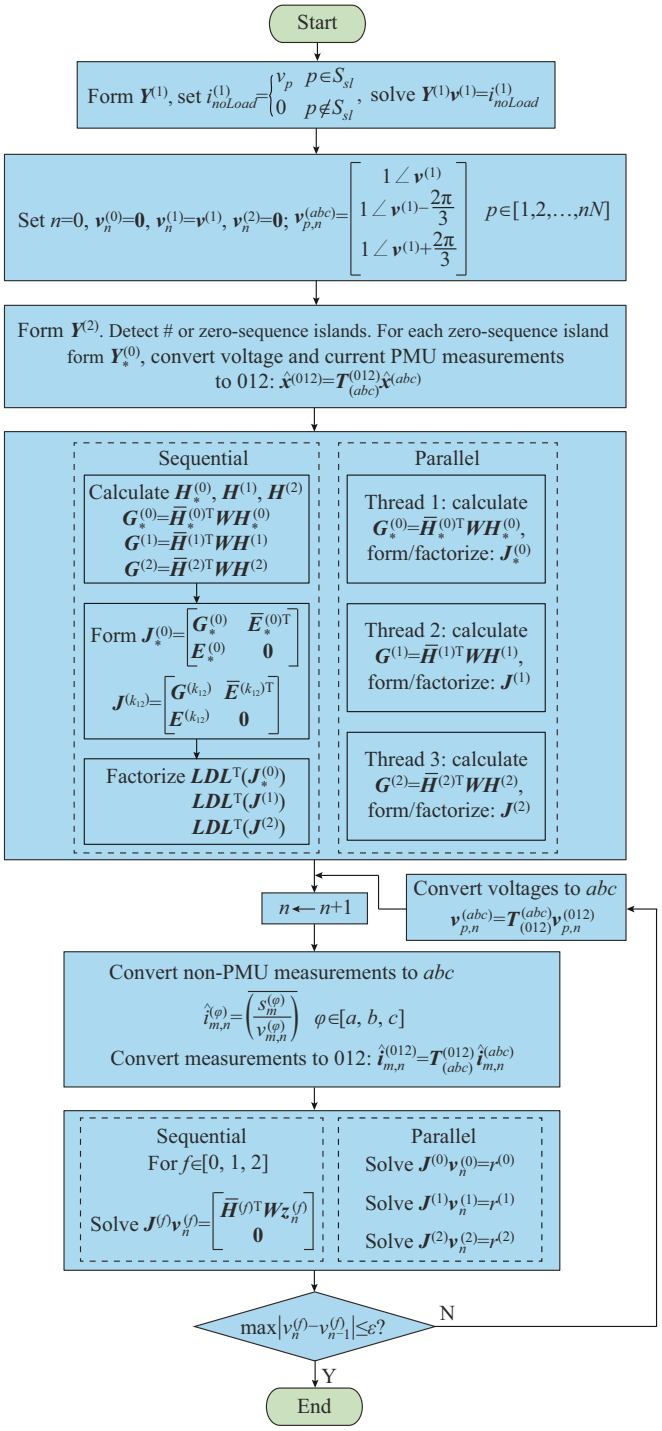

Fig. 1. Sequential and parallel PGNSE algorithm using Fortescue transformation.

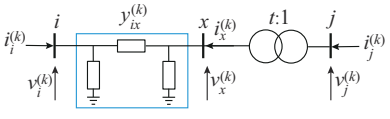

Fig. 2. General π-equivalent transformer model.

$$\begin{bmatrix}y_{ii}^{(1)} & -y_{ix}^{(1)}t\\ -\bar{t}y_{xi}^{(1)} & |t|^2y_{xx}^{(1)}\end{bmatrix}\begin{bmatrix}v_i^{(1)}\\ v_j^{(1)}\end{bmatrix}=\begin{bmatrix}i_i^{(1)}\\ i_j^{(1)}\end{bmatrix} \tag{16}$$

The positive- and negative-sequence π-equivalent circuits

have the same impedance values but different clock numbers. In the case of negative sequence, the clock number is negative, and the corresponding negative-sequence nodal equations for the circuit in Fig. 2 are given by (17). The same positive- and negative-sequence circuits apply to the delta-delta connection ($c = 0, 2, 4, 6, 8, 10$).

$$\begin{bmatrix} y_{ii}^{(1)} & -y_{ix}^{(1)}\bar{t} \\ -ty_{xi}^{(1)} & |t|^2 y_{xx}^{(1)} \end{bmatrix} \begin{bmatrix} v_i^{(2)} \\ v_j^{(2)} \end{bmatrix} = \begin{bmatrix} i_i^{(2)} \\ i_j^{(2)} \end{bmatrix} \tag{17}$$

B. Zero-sequence Transformer Circuit

The zero-sequence circuit of the transformer is affected by the winding connections and the type of grounding. For example, for the wye-wye connection with grounded g primary and secondary, i.e., $Y_g y_g 0$ and $Y_g y_g 6$, the circuit model in Fig. 2 still holds but generally has different impedance values. The corresponding nodal equations are the same form as (16) but employ zero-sequence quantities. However, the wye-delta and delta-wye connections with a grounded wye-winding, i.e., $Y_g dc$ and $Dy_g c$ ($c = 1, 5, 7, 11$), behave as a zero-sequence filter. As shown in Fig. 3, the clock number does not play a role in the corresponding zero-sequence circuits. Other transformer configurations (those involving a wye-connected winding without grounding and the delta-delta connection) introduce an open circuit for zero-sequence currents on both terminals.

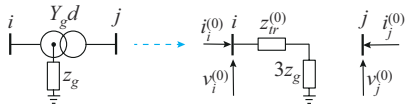

Fig. 3. Wye grounded-delta transformer connection.

IV. Zero-sequence Islands

The zero-sequence transmission network could cause ill-conditioning of the whole calculation process in both Fortescue and phase-coordinates calculations. In the phase-coordinate approach [7], the ill-conditioning problem is typically solved by adding shunt elements at delta windings which are then compensated by fictitious current generators [19]. Another method for treating ill-conditioning is shown in [17], [19] by embedding a methodology for changing critical pivot values during the factorization phase. The obtained matrix is indefinity for equality-constrained state estimation, necessitating a special pivoting strategy involving 1×1 and 2×2 pivots. This procedure is extremely difficult because it requires the use of a non-standard sparse matrix solver. It may also affect the results in cases where the system is on the verge of black-out. This letter proposes a graph-based algorithm for removing the source of ill-conditioning while speeding up the solution process. Consider the illustrative example in Fig. 4. Figure 5 is obtained after applying the zero-sequence line and transformer models, where it is visible that areas I and IV can easily pass the zero-sequence current. Area II can conduct only the minimal capacitive zero-sequence currents. However, since the system admittance matrix of area III is singular, it would cause the whole system admittance matrix to become singular. Therefore, instead of calculating a single zero-sequence admittance matrix, a separate zero-sequence admittance matrix is defined for every zero-sequence connected island. For those islands where the zero-sequence admittance matrix cannot be inverted, the zero-sequence currents are equal to null. Thus, there is no need to estimate the zero-sequence values in such areas. The singularity is wholly removed without introducing any ill-conditioning to the rest of the system. The analysis requires the creation of one system admittance matrix for positive-sequence ($k = 1$), one system admittance matrix for negative-sequence ($k = 2$), and a set of system admittance matrices after a topological trace of the equivalent zero-sequence network [20]. Algorithm 1 summarizes the graph-based procedure for the detection of zero-sequence islands. The algorithm employs the non-recursive breadth-first search method, as defined in [20], [21]. Each zero-sequence island will be assigned a unique identifier (color), which will be used to compute the corresponding matrices. The corresponding Jacobian and zero-sequence gain matrices for the areas that require estimation are marked with an asterisk sign "*" in the numerical algorithm of Fig. 1. *Xfmr* stands for transformer.

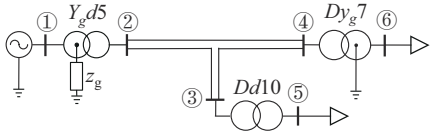

Fig. 4. Symmetrical transmission system with different three-phase transformer connections.

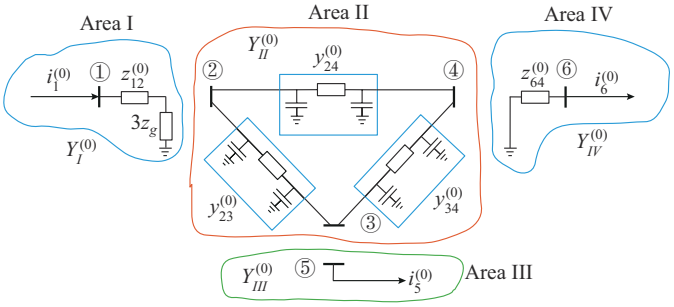

Fig. 5. Equivalent zero-sequence network.

Algorithm 1: graph-based procedure for detection of zero-sequence island

```
Create graph G = graph(i,j);
C = {slackNode}, color(k) ← 0, k = 1, 2, …, nN;
islandNo ← 0, i ← slackNode;
do
  i ← dequeue(C), islandNo ← islandNo + 1;
  color(i) ← islandNo, A ← adjacentNodes(G(i));
  while A is not empty
    j ← dequeue(A) //A = A − {j}
    if color(j) <> 0 continue;
    if conn(ij) = Xfmr and connType <> Ygyg
      C ← C + {j}, continue;
    A ← A + adjacentNodes(G(j)), color(j) ← islandNo;
  end while
  C ← {C:color(C(k)) = 0, k = 1, 2, …, dim(C)};
while C is not empty
```

V. Numerical Results

Tests were carried out using transmission networks (118, 1888, and 9241 three-phase nodes) and European distribution networks (1500 and 3000 three-phase nodes). The IEEE 118-, 1888-, and 9241-bus test systems are available with the MATPOWER distribution files from [22]. The 1k5 and 3k distribution network instances are described in [23] and their data are available from [24]. The number of measurements is expressed via three-phase measurement points. Table I shows the three single-phase measurements for complex power (S), phasor measurement unit currents (PMUI), and voltages (PMUV). The calculation time is averaged over ten solutions of the PGNSE algorithm in Fig. 1 in both the sequential (Seq.) and parallel (Par.) implementations and compared with the vectorized-code implementation of the phase-coordinates approach (MPh.) [7]. The computations are done from a flat start (factorization+backward/forward iterations) on a MacBook with a 4-core Intel Processor 1.8 GHz and 8 GB RAM. The proposed PGNSE algorithm based on Fortescue transformation gives a speed-up factor (SUF) relative to [7] (SUF is the ratio of the time of MPh. to the time of PGNSE), which is about three for the sequential implementation and five for the parallel one as shown in Table I. The maximum percentage of voltage deviation is also shown in Table I: $\Delta V = \max\{100 \times |(v_i - vr_i)/vr_i|\}$, where vr_i and v_i are the complex voltages at node i calculated by [7] and the method described in this letter, respectively. Since the maximum deviation is less than 0.1%, both the proposed PGNSE algorithm and the compensation-based phase-coordinates approach provide solutions with the same accuracy.

TABLE I
Numerical Results

Network	Number of three-phase measurements			Calculation time (ms)			ΔV (%)	SUF	
	S	PMUI	PMUV	MPh. [7]	Seq.	Par.		Seq.	Par.
118A	186	186	3	41.6	13.7	8.6	0.02	3.0	4.9
118B	0	186	118	12.8	4.5	2.9	0	2.8	4.4
1k5A	1286	648	735	415.7	134.8	83.9	0.03	3.1	5.0
1k5B	0	1948	1426	119.7	39.7	24.8	0	3.0	4.8
1888A	2531	1261	87	637.0	208.9	124.9	0.05	3.0	5.1
1888B	0	2531	1888	148.9	50.3	30.6	0	3.0	4.9
3kA	2228	1898	2534	1304.2	458.7	263.3	0.05	2.8	5.0
3kB	0	3386	2986	358.1	122.1	72.6	0.00	2.9	4.9
9241A	16049	8025	66	3305.6	1097.2	635.3	0.07	3.0	5.2
9241B	0	16049	9241	529.5	171.7	102.1	0.01	3.1	5.2

Test results are obtained on an 1888A network instance with isolated areas under increased loading, and the convergence pattern of phase-coordinates and estimators based on Fortescue transformation are summarized in Table II. Measurements were generated by multiplying each load by the load multiplier coefficient. Because of the singularity isolation feature, the proposed algorithm can be used to solve the system under higher loading conditions.

TABLE II
Convergence Pattern of Phase-coordinates and Estimators Based on Fortescue Transformation on 1888A Network ($\varepsilon = 10^{-6}$)

Load multiplier	Solution status	
	Phase-coordinates [7]	Fortescue
1.000	Converged	Converged
1.050	Converged	Converged
1.060	Converged	Converged
1.066	Converged	Converged
1.067	Failed	Converged
1.070	Failed	Converged
1.072	Failed	Converged

VI. Conclusion

Recent research has shown the advantage of estimation based on Fortescue transformation, but presented findings limited to the measurements from PMUs. This letter demonstrated that better numerical conditions and a significant speed-up could be obtained from the estimator based on Fortescue transformation compared with the standard phase-coordinates implementation even with classical SCADA measurements when the computation exploits the recent PGNE framework.

References

[1] R. A. Jabr and I. Dzafic, "Distribution management systems for Smart Grid: Architecture, work flows, and interoperability," *Journal of Modern Power Systems and Clean Energy*, vol. 10, no. 2, pp. 300-308, Mar. 2022.

[2] M. Göl and A. Abur, "A robust PMU based three-phase state estimator using modal decoupling," *IEEE Transactions on Power Systems*, vol. 29, pp. 2292-2299, Sept. 2014.

[3] R. Khalili and A. Abur, "PMU-based decoupled state estimation for unsymmetrical power systems," *IEEE Transactions on Power Systems*, vol. 36, pp. 5359-5368, Nov. 2021.

[4] T. R. Fernandes, B. Venkatesh, and M. C. de Almeida, "Symmetrical components based state estimator for power distribution systems," *IEEE Transactions on Power Systems*, vol. 36, no. 3, pp. 2035-2045, May 2021.

[5] I. Džafić, R. A. Jabr, and T. Hrnjić, "A complex variable perturbed Gauss-Newton method for tracking mode state estimation," *IEEE Transactions on Power Systems*, vol. 36, pp. 2594-2602, May 2021.

[6] V. Murugesan, Y. Chakhchoukh, V. Vittal *et al.*, "PMU data buffering for power system state estimators," *IEEE Power and Energy Technology Systems Journal*, vol. 2, pp. 94-102, Sept. 2015.

[7] I. Džafić, R. A. Jabr, and T. Hrnjić, "Complex variable multiphase distribution system state estimation using vectorized code," *Journal of Modern Power Systems and Clean Energy*, vol. 8, no. 4, pp. 679-688, Jul. 2020.

[8] I. Roytelman and J. M. Palomo, *Volt/VAR Control in Distribution Systems - IET Power and Energy Series: Power Distribution Automation*. London: IET Press, 2016.

[9] I. Džafić, B. C. Pal, M. Gilles *et al.*, "Generalized π Fortescue equivalent admittance matrix approach to power flow solution," *IEEE Transactions on Power Systems*, vol. 29, no. 1, pp. 193-202, Jan. 2014.

[10] R. A. Jabr and I. Džafić, "A Fortescue approach for real-time short circuit computation in multiphase distribution networks," *IEEE Transactions on Power Systems*, vol. 30, no. 6, pp. 3276-3285, Nov. 2015.

[11] M. Abdel-Akher and K. M. Nor, "Fault analysis of multiphase distribution systems using symmetrical components," *IEEE Transactions on Power Delivery*, vol. 25, no. 4, pp. 2931-2939, Oct. 2010.

[12] I. Džafić and R. A. Jabr, "Real-time equality-constrained hybrid state estimation in complex variables," *International Journal of Electrical Power & Energy Systems*, vol. 117, p. 105634, May 2020.

[13] A. Ahmadi, M. C. Smith, E. R. Collins *et al.*, "Fast Newton-Raphson power flow analysis based on sparse techniques and parallel process-

ing," *IEEE Transactions on Power Systems*, vol. 37, no. 3, pp. 1695-1705, May 2021.
[14] A. Leon-Garcia, *Probability, Statistics, and Random Processes for Electrical Engineering*. Upper Saddle River: Pearson, 2008.
[15] R. Singh, B. C. Pal, and R. A. Jabr, "Choice of estimator for distribution system state estimation," *IET Generation, Transmission & Distribution*, vol. 3, no. 7, pp. 666-678, Aug. 2009.
[16] M. C. de Almeida and L. F. Ochoa, "An improved three-phase AMB distribution system state estimator," *IEEE Transactions on Power Systems*, vol. 32, no. 2, pp. 1463-1473, Mar. 2017.
[17] D. Anderson and B. Wollenberg, "Solving for three phase conductively isolated busbar voltages using phase component analysis," *IEEE Transactions on Power Systems*, vol. 10, no. 1, pp. 98-108, Feb. 1995.
[18] I. Džafić, R. A. Jabr, and H.-T. Neisius, "Transformer modeling for three-phase distribution network analysis," *IEEE Transactions on Power Systems*, vol. 30, no. 5, pp. 2604-2611, Sept. 2015.
[19] T. R. Fernandes, T. R. Ricciardi, R. S. da Silva *et al.*, "Contributions to the sequence-decoupling compensation power flow method for distribution system analysis," *IET Generation, Transmission & Distribution*, vol. 13, no. 5, pp. 583-594, Mar. 2019.
[20] R. Sedgewick, *Algorithms in C*. Reading: Addison-Wesley Publishing Company, 1990.
[21] I. Džafić, "Graph theory as an engine for real-time advanced distribution management system enhancements," in *Proceedings of 28th International Conference on Information, Communication and Automation Technologies (ICAT 2022)*, Sarajevo, Bosnia and Herzegovina, Jun. 2022, pp. 1-6.
[22] C. Josz, S. Fliscounakis, J. Maeght *et al.* (2016, Mar.). AC power flow data in MATPOWER and QCQP format: iTesla, RTE snapshots, and PEGASE. [Online]. Available: https://arxiv.org/abs/1603.01533v3
[23] R. A. Jabr and I. Džafić, "Sensitivity-based discrete coordinate-descent for Volt/VAr control in distribution networks," *IEEE Transactions on Power Systems*, vol. 31, no. 6, pp. 4670-4678, Nov. 2016.
[24] R. A. Jabr and I. Džafić. (2022, Jun.). VVC distribution network data sets. [Online]. Available: https://www.dropbox.com/s/2ug5noo4or4dch8/VVC_DistNets.7z?dl=0

Izudin Džafić received the Ph. D. degree from University of Zagreb, Zagreb, Croatia, in 2002. He is currently a Professor in the Department of Automatic Control and Electronics, Faculty of Electrical Engineering, University of Sarajevo, Sarajevo, Bosnia and Herzegovina. From 2002 to 2014, he was with Siemens AG, Nuremberg, Germany, where he held the position of the Head of the Department and Chief Product Owner (CPO) for Distribution Network Analysis (DNA) R&D. He holds 15 US and international patents. He is a member of the IEEE Power and Energy Society and the IEEE Computer Society. His research interests include power system modeling, development and application of fast computing to power system simulations.